XinJiaCongRongTuSiZiWan Protects TP-Induced Rats from Oxidative Stress Injury via Mitophagy Mediated PINK1/ Parkin Signaling Pathway

Jin Yan
Shaanxi University of Chinese Medicine
Disi Deng
Hospital of Chengdu University of Traditional Chinese Medicine
Min Liu
Hospital of Chengdu University of Traditional Chinese Medicine
Yeke Wu
Hospital of Chengdu University of Traditional Chinese Medicine
Keming Wu (wu_keming1@126.com)
Hospital of Chengdu University of Traditional Chinese Medicine

Research

Keywords: Triptolide, XinJiaCongRongTuSiZiWan, reproductive toxicity, oxidative stress, mitophagy, PINK1, Parkin

Posted Date: October 28th, 2021

DOI: https://doi.org/10.21203/rs.3.rs-990305/v1

Abstract

Background: Oxidative stress is one of main molecular mechanisms involved in toxicity of triptolide (TP). Although our group has discovered the effectiveness of XinJiaCongRongTuSiZiWan (XJCRTSZW) on premature ovarian failure (POF) and polycystic ovary syndrome (PCOS), whether the protective role of XJCRTSZW being associated with oxidative stress is still totally understood.

Methods: Adult female Sprague-Dawley rats and human ovarian granulosa cell lines were treated with TP, and then treated with XinJiaCongRongTuSiZiWan (XJCRTSZW). Histological analysis and follicle count were executed using H&E staining. Hormone (E2, AMH, P, FSH and LH) concentrations, oxidative stress indicators (SOD and MDA), apoptosis rate, ATP content, mitochondrial membrane potential (MMP), cell viability, mitophagy and relative mRNA and protein levels (LC3-Ⅱ/LC3-Ⅰ, p62, Hsp60, PINK1 and Parkin) were detected by ELISA, commercial biochemical detection kits, flow cytometry, JC-1 staining, CCK-8, transmission electron microscope and western blotting respectively.

Results: XJCRTSZW treatment observably ameliorated the TP-induced the pathological symptoms, including the decreased primordial follicles, primary follicles and secondary follicles numbers in the cortical area, the increased numbers of atretic follicles, necrotic and shedding, and nuclear constriction and collapse with cystic dilatation *in vivo*. Furthermore, XJCRTSZW treatment observably enhanced the TP-induced reduction of E2, AMH and P concentrations, SOD concentrations, ATP content, MMP, p62 and Hsp60 mRNA and protein level, but, diminished the TP-induced elevation of FSH and LH concentrations, MDA level, ROS level, apoptosis rate, mitophagy, and the mRNA and protein expression of LC3-Ⅱ/LC3-Ⅰ, PINK1 and Parkin both *in vivo* and *in vitro*. In addition, XJCRTSZW treatment markedly increased the TP-induced reduction of cell viability *in vitro*.

Conclusion: XinJiaCongRongTuSiZiWan protects TP-induced rats from oxidative stress injury via mitophagy mediated PINK1/ Parkin signaling pathway.

Background

Triptolide (TP), a diterpene trioxide, is a major component extracted from Chinese herb *Tripterygium wilfordii* Hook F [1], which has been widely used for the treatment of autoimmune, inflammatory diseases and variety of tumors [2–4]. However, plenty of studies have exhibited the severe reproductive system toxicity in TP-treated animals and patients [5, 6]. Oxidative stress is one of core molecular mechanisms involved in toxicity of TP that has been demonstrated to be tightly associated with follicular atresia and ovulation disorders including premature ovarian failure (POF) and polycystic ovary syndrome (PCOS) [7, 8]. Therefore, oxidative stress may be the plausible target for the prevention or treatment of TP-induced reproductive toxicity, and pharmacologic oxidative stress modulators can be the promising drug candidates.

Except for apoptosis, a major hallmark for the TP-induced reproductive toxicity, other forms of programmed cell death (PCD) such as autophagy can also be activated primarily in granulosa cells (GCs)

[7]. Autophagy is a highly conserved and closely modulated process that transports cellular substrates to lysosomes for bulk degradation that comprises macroautophagy, mitophagy and chaperone-mediated autophagy. Among them, mitophagy degrades the damaged mitochondria that acts as an effector of PCD and promotes cell death programs. Moreover, previous study has revealed that oxidative stress-induced mitochondrial permeability transition induces the depolarization of mitochondrial membrane potential, which leads to the PTEN-induced kinase 1 (PINK1) accumulation on the outer mitochondrial membrane. Subsequently, PINK1 recruits Parkin, a E3 ubiquitin ligase, to begin the autophagic degradation of damaged mitochondria23–25. Thus, mitophagy may play an important role in the TP-induced oxidative stress response.

XinJiaCongRongTuSiZiWan (XJCRTSZW) is a traditional Chinese medicine (TCM) compound for invigorating the kidney, nourishing blood and promoting blood circulation, which is created by Professor Keming Wu according to many years of clinical experience. The prescription contains Cistanche, Cuscuta, Raspberry, Morus, Rehmannia, Angelica, Epimedium, Caulis Spatholobi, Cyperus rotundus, Fructus Leonuri, Wolfberry, Eupatorium, Chinese Yam, and Dogwood. Cistanche, Cuscuta and Raspberry are functioned as the emperor medicines to invigorate the kidney and essence. Epimedium, Dogwood, and Rehmannia act as minister medicines to strengthen the power of the emperor medicines to nourish the kidney. Among them, Epimedium warms the kidney and yang, and Rehmannia and Dogwood nourish the essence and blood of liver and kidney. The rest of the medicines is all adjuvants. Among them, Angelica, Caulis Spatholobi, Fructus Leonuri, Wolfberry and Eupatorium nourish blood and promote blood circulation; Morus nourishes the liver and kidneys, strengthens muscles and bones; Chinese Yam nourishes qi and invigorates the spleen; and Cyperus rotundus is the key to regulating menstruation in gynecology, which can regulate the qi and activate the blood, and make all the medicines tonic without stagnation. Our group have been discovered that the effective treatment of XJCRTSZW on POF [9] and PCOS [10]. Furthermore, our previous results have also shown that XJCRTSZW reduce the TP-induced enhancement of apoptosis and macroautophagy. However, the role of XJCRTSZW on the TP-induced oxidative stress mediated by mitophagy is still not fully understood.

Therefore, in the present study, we found that XJCRTSZW can ameliorate TP-induced oxidative stress through mitophagy both *in vivo* and *in vitro*. Mechanically, mitophagy mediated by PINK1/ Parkin signaling pathway is involved in this process both *in vivo* and *in vitro*. The results of this study will provide new sights and methods for the therapy of reproductive toxicity, even for POF and PCOS.

Materials And Methods

Animal

Adult female Sprague-Dawley rats (7-8 weeks, 200–220 g) were bought from Chengdu Dashuo Biological Technology Co., Ltd., Rats were acclimated to standard laboratory conditions for 7 days before experiments. Rats were supplied with a 12 hour/12 h light-dark cycle and fed with standard diet and water *ad libitum* with (25 ± 2) ℃, and 40%-60% the relative humidity. All the procedures were executed

severely according to the Board and Ethics Committee of Chengdu University of Traditional Chinese Medicine.

Cell culture

Human ovarian granulosa cell lines (cat no. CP-H192) were bought from Procell (Wuhan, China). Cells were cultured in complete medium for human ovarian granulosa cells (CM-H192, Procell) at 37°C with 5% carbon dioxide (CO_2).

Cell transfection

Pink1 mimics and Pink1 inhibitor were designed and synthesized by Ribobio (Guangzhou, China). It was performed with RiboFectTM CP Transfection Kit (C10511-05, Ribobio) based on the experimental procedures for the following assays.

Preparation of medicated serum

For *in vitro* experiments, medicated serum was first prepared as following description. 15 rats were randomly divided into three groups (n=5), including control, estradiol valerate (EV, western medicine control group) and XJCRTSZW group. Rats in EV group were intragastrically administered with 0.105 mg/(kg.d) EV once a day for 4 consecutive days, and then with 0.63 mg/(kg.d) medroxyprogesterone acetate once a day for one day. Rats in XJCRTSZW group were intragastrically administered with 23.1437 g/(kg.d) XJCRTSZW, while rats in control group were intragastrically administered with 1ml/100g saline 2 times a day for 5 consecutive days. Subsequently, blood was obtained from the abdominal aorta after the rats were intraperitoneally anesthetized with sodium pentobarbital (40 mg/kg). Serum was isolated and inactivated the complement for *in vitro* experiments.

Experimental groups and drug administration

For *in vivo* experiments, 30 rats were randomly divided into six groups (n=5), including control, TP, TP+EV, TP+XJCRTSZW-High, TP+XJCRTSZW-Middle and TP+XJCRTSZW-Low. Rats in TP, TP+EV, TP+XJCRTSZW-High, TP+XJCRTSZW-Middle and TP+XJCRTSZW-Low group were intragastrically administered with 400 μg/kg.d TP (dissolved in saline containing 5% DMSO) for continuous 30 days to induce the reproductive toxicity, while rats in control group were intragastrically administered with equal amount of saline. Then, rats in TP+XJCRTSZW-High, TP+XJCRTSZW-Middle and TP+XJCRTSZW-Low group were intragastrically administered 23.1437 g/(kg.d), 11.5718 g/(kg.d) and 5.7859 g/(kg.d) XJCRTSZW respectively for 2 weeks. Rats in TP+EV group were intragastrically administered with 0.1 mg/(kg.d) EV once a day for 4 consecutive days, and then with 0.598 mg/(kg.d) medroxyprogesterone acetate once a day for one day. A total of 15 days continued with 1 day after stopping the drug. Rats in control and TP group were intragastrically administered with 1ml/100g saline once a day, for 2 weeks. The total amount of crude drug of XJCRTSZW per dose is 115 g, which is made into an extract by the Department of Pharmacy of Chengdu University of Traditional Chinese Medicine. The concentration of XJCRTSZW in high, middle and low group, as well as EV and medroxyprogesterone acetate was determined according to the adult clinical dose of 6 kg per kilogram of body weight and the ratio of

human to rat being 1:20 for conversion. After the rats were intraperitoneally anesthetized with sodium pentobarbital (40 mg/kg), blood was taken from the abdominal aorta. Serum was isolated and stored at -80°C for further assays. Ovary tissues and GCs were fleetly removed for subsequent analysis.

For *in vitro* experiments, human ovarian granulosa cell lines were inoculated into six-well plates and divided into eight groups including control, TP, TP+EV, TP+XJCRTSZW, TP+XJCRTSZW+si-Pink1, TP+XJCRTSZW+ov-Pink1, TP+ si-Pink1 and TP+ ov-Pink1 groups. Human ovarian granulosa cells in control group were cultured in complete medium for human ovarian granulosa cells, while cells in the other seven groups were cultured in complete medium for human ovarian granulosa cells including 100 nM TP for 6 h. Then, cells in TP group were cultured in complete medium for human ovarian granulosa cells including 200 μL control serum obtained from control rats, while cells in TP+EV group were cultured in complete medium for human ovarian granulosa cells including 200 μL EV serum obtained from EV rats as 2.4 described. Cells in TP+XJCRTSZW, TP+XJCRTSZW+si-Pink1, TP+XJCRTSZW+ov-Pink1 groups were cultured in complete medium for human ovarian granulosa cells including 200 μL medicated serum obtained from rats in XJCRTSZW group described in 2.4 above. Subsequently, cells in TP+XJCRTSZW+si-Pink1, TP+XJCRTSZW+ov-Pink1 groups were cultured in complete medium for human ovarian granulosa cells including 20 nM Pink1 inhibitor and 2 μg Pink1 mimics respectively. Cells in TP+ si-Pink1 and TP+ ov-Pink1 groups were cultured in complete medium for human ovarian granulosa cells including 200 μL control serum obtained from control rats, as well as 20 nM Pink1 inhibitor and 2 μg Pink1 mimics respectively. Cells were maintained at 37°C with 5% carbon dioxide (CO_2) for further 48 h.

Cell Counting Kit-8 assay

Human ovarian granulosa cells were cultured in 96-well plates with a inoculation density of 1×10^5/well and maintained for 24 h at 37°C in 5% CO_2. Then, the Cell Count Kit-8 (Dojindo Laboratories, Kumamoto, Japan) was utilized to determine the proliferation of cells based on the manufacturer's specifications. The absorbance was recorded at 450 nm uisng a microplate reader (Thermo Fisher Scientific, Waltham, MA, USA).

Histological assays and follicle count

The ovarian tissue was separated, fixed, decalcified, embedded and cut into sections. 5 μm sections were stained with hematoxylin and eosin (H&E). Pictures were obtained under a microscope (DMI1, LEICA, Germany). Then, the number of primary follicles, secondary follicles and atretic follicle was measured.

Enzyme-linked immunosorbent assay (ELISA)

The levels of estradiol (E2), anti-Mullerian hormone (AMH), follicle stimulating hormone (FSH), luteinizing hormone (LH), Progesterone (P) and ATP were detected using Estradiol ELISA Kit (PE223, Beyotime, Shanghai, China), Rat anti-Mullerian hormone (AMH) ELISA KIT (YB-AMH-Ra, Ybscience, Shanghai, China), Rat Follicle Stimulating Hormone (FSH) ELISA KIT (XY-FSH-Ra, Ybscience), Rat luteinizing hormone (LH) ELISA KIT (XY-LH-Ra, Ybscience), Rat Progesterone, PROG ELISA kit (KB3091, Kemin Biology, Shanghai, China) and Rat ATP ELISA KIT (made by Qingqi Biology, Shanghai, China) according

to the manufacturer's protocol. The absorbance of wells was determined with a microplate reader (Thermo Fisher Scientific) at 450 nm wave length to analyze the sample concentration.

Biochemical detection

The levels of malondialdehyde (MDA) and superoxide dismutase (SOD) were detected using Lipid Peroxidation MDA Assay Kit (S0131M, Beyotime) and Total Superoxide Dismutase Assay Kit with NBT (S0109, Beyotime) according to the manufacturer's protocol. The absorbance of wells was determined with a microplate reader (Thermo Fisher Scientific) at 532 nm (MDA) and 560 nm (SOD) wave length to analyze the sample concentration.

Flow cytometric assay

Apoptosis of GCs was evaluated using flow cytometric assay. In brief, GCs were collected and stained with Annexin V-APC and PI (Sigma Aldrich, St. Louis, MO, USA) at room temperature for 20 min in the dark. The fluorescence of the cells was measured by flow cytometry (BD FACSVerse, Waltham, MA, USA).

The level of ROS was detected using Reactive oxygen species assay kit (S0033, Beyotime, Shanghai, China) based on the operating manual. The fluorescence of the cells was measured by flow cytometry (BD FACSVerse).

JC-1 staining

GCs cultured on coverslips were maintained with 0.1 μM JC-1 (Molecular Probes) at 37°C for 20 min. Fluorescence images were obtained by a laser-scanning confocal microscope (Zeiss LSM 710 META) with an excitation at 525 nm and 490 nm respectively. CCCP (50 mM) was used as a positive control and treated for 20 min before JC-1 staining. Changes of mitochondrial membrane potential (MMP) were analyzed by the ratio of aggregated JC-1 (525 nm, red fluorescence) to monomeric JC-1 (490 nm, green fluorescence).

Transmission electron microscopy

Ovary tissues and GCs were fixed in 3% glutaraldehyde and 1% osmium tetroxide and cut on an ultramicrotome. Then sections were stained with 1% uranyl acetate and 0.5% lead citrate successively. The results were observed using JEM-1400PLUS transmission electron microscope.

Reverse transcription-quantitative polymerase chain reaction (RT-qPCR) analysis

Total RNA was isolated using TRIzol reagent (TaKaRa Biotechnology Co., Ltd., Dalian, China) and RT was conducted by Bio-Rad ScripTM cDNA Synthesis Kit (Bio-Rad Laboratories, Inc., Hercules, CA, USA) according to the manufacturer's instructions. The resulting RT products were stored at -80°C until analysis. RT-qPCR was performed in a 20-μl mixture containing 2 μl of the cDNA templates, 10 μl 2x SYBR Master mix (MedChemexpress, Princeton, NJ, USA), 0.4 μl of the 10-μM forward and reverse primers and

7.2 μl ddH2O, using the Bio-Rad CFX Manager software (Bio-Rad Laboratories, Inc.). The RT-qPCR conditions were as follows: 5 min at 95°C, followed by 40 cycles between 95°C for 15 sec and 60°C for 30 sec, and 72°C for 30 sec. The relative expressions of LC3, PINK1, Parkin, p62 and Hsp60 were calculated using the 2-ΔΔCT method and normalized to the housekeeping gene β-actin. The primer sequences (Sangon Biotech Co., Ltd., Shanghai, China) are listed in Table I. For the quantification of miR-122 expression, the RT reaction was performed using Bulge-Loop™ miRNA RT-qPCR Primer (RiboBio Co., Ltd., Guangzhou, China). The RT reaction was processed at 42°C for 60 min and at 70°C for 10 min. Gene expression levels were quantified at 95°C for 10 min, followed by 40 cycles at 95°C for 2 sec, 60°C for 20 sec and 70°C for 10 sec. U6 served as the internal control.

Western blot assay

Protein samples from GCs separated from ovary or human ovarian granulosa cells were extracted using a Total Protein Extraction Kit (BC3711, Solarbio, Beijing, China). Then, the protein concentration was detected by a Protein Assay kit (Beyotime). Next, protein samples were separated by 10% SDS-PAGE gel and electrically transferred to PVDF membranes (Millipore, MA, USA). After blocked with 3% bovine serum albumin (BSA) for 1 h at room temperature, the membranes were incubated with the primary antibodies at 4℃ overnight. After washing with TBST for 3×5 min, the membranes were incubated with goat-anti-rabbit IgG (H+L)-HRP (1:10000, ab6721, Abcam, Cambridge, UK) for 1 h at room temperature. Protein bands were analyzed by an Electrochemilluminescence (ECL) chemiluminescence kit (WBULS0500; EMD Millipore) and the bands intensity was quantified with Image-Pro Plus 6.0 software. The primary antibodies used were as follows: rabbit anti-LC3II/I (ab128025; 1: 1,000), rabbit anti-p62 (ab56416; 1: 1,000), Rabbit polyclonal to PINK1 (ab23707; 1: 1,000), Rabbit polyclonal to Parkin (ab15494; 1: 1,000), Rabbit polyclonal to Hsp60 (ab46798; 1: 2,0000), and rabbit anti-β-actin (ab8227; 1: 1,000).

Statistical analysis

Data were presented as the means ± standard deviation. Differences among multiple groups were analyzed using one-way analysis of variance and Duncan's test using the SPSS 20.0 package (SPSS Inc. Chicago, IL, USA). The differences were considered as statistically non-significant and significant when $p > 0.05$ and $p < 0.05$, respectively.

Results

XJCRTSZW ameliorates TP-induced reproductive toxicity in vivo

After rats were treated with TP, pathological analysis revealed that the number of primordial follicles, primary follicles and secondary follicles in the cortical area was decreased, while the number of atretic follicles was increased. Moreover, some granular layer follicles were necrotic and shedding, and nuclear constriction and collapse were seen with various degrees of cystic dilatation. However, these pathological symptoms were notably improved with both EV and XJCRTSZW treatment (Fig. 1A). Furthermore, quantification of follicle numbers showed that both EV and XJCRTSZW treatment significantly enhanced the TP-induced the reduction of primary follicles and secondary follicles numbers, while prominently

decreased the TP-induced the elevation of atretic follicle numbers (Fig. 1B and C). The serum levels of E2 and AMH were observably diminished, whereas these of FSH and LH were markedly increased with TP treatment. However, both EV and XJCRTSZW treatment prominently reversed the decrease of E2 and AMH levels, while only XJCRTSZW treatment significantly antagonized the enhancement of FSH and LH levels (Fig. 1D). Taken together, we demonstrated that XJCRTSZW ameliorates TP-induced reproductive toxicity in the rat model.

XJCRTSZW inhibits TP-induced oxidative stress injury in vivo

To determine the role of XJCRTSZW in TP-induced oxidative stress injury, we first detected the level of SOD and MDA. The results showed that all the EV, high and middle-does XJCRTSZW treatment significantly elevated the TP-induced the diminishment of SOD levels, while only EV and high-does XJCRTSZW treatment prominently inhibited the TP-induced enhancement of MDA levels (Fig. 2A). In addition, all the EV, high, middle and low-does XJCRTSZW treatment notably antagonized the TP-induced the increase of ROS levels (Fig. 2B). Furthermore, TP treatment markedly enhanced the apoptosis rate of GCs, which was observably reversed with all the EV, high, middle and low-does XJCRTSZW treatment (Fig. 2C and D). Therefore, these results suggested that XJCRTSZW inhibits TP-induced oxidative stress injury and apoptosis *in vivo*.

XJCRTSZW promotes TP-induced mitophagy via PINK1/ Parkin signaling pathway in vivo

Transmission electron microscopy showed a large number of swollen mitochondria in GCs with broken, dissolved or even disappeared cristae, and a spot of mitophagy in TP treatment group, while the EV, high, middle and low-does XJCRTSZW treatment relieved the degree of mitochondrial swelling and increased the number of mitophagy (Fig. 3A). Besides, the levels of ATP and MMP were observably reduced with TP treatment, which were markedly rescued with EV and high-does XJCRTSZW treatment (Fig. 3B and C). Both EV and high-does XJCRTSZW treatment prominently increased the LCII/LCI expression, while significantly decreased the p62 and Hsp60 expression both at transcriptional and translational levels compared to these in TP group (Fig. 3D, E and F). Furthermore, the mRNA and protein expression levels of PINK1 and Parkin were notably enhanced with both EV and high-does XJCRTSZW treatment compared to these in TP group. Altogether, we concluded that XJCRTSZW promoted TP-induced mitophagy via PINK1/ Parkin signaling pathway *in vivo*.

XJCRTSZW promotes the cell viability of GCs induced by TP

The cell viability of human ovarian granulosa cells was notably declined with TP treatment, which was prominently rescued with EV or XJCRTSZW treatment. Moreover, further inhibition or overexpression of PINK1 prominently decreased and increased the cell viability based on the XJCRTSZW-induced enhancement respectively. Only inhibition or overexpression of PINK1 markedly reduced or elevated the cell viability compared to that in TP group respectively (Fig. 4A). Similarly, EV or XJCRTSZW treatment

notably increased the TP-induced reduction of E2, AMH and P level in supernatant of cultured human ovarian granulosa cells. XJCRTSZW treatment combined with inhibition or overexpression of PINK1 further markedly diminished the TP-induced enhancement, or increased the TP-induced reduction of E2, AMH and P level in supernatant of cultured human ovarian granulosa cells. On the contrary, EV or XJCRTSZW treatment notably decreased the TP-induced elevation of E2, AMH and P level in supernatant of cultured human ovarian granulosa cells. XJCRTSZW treatment combined with inhibition or overexpression of PINK1 further markedly enhanced the TP-induced diminishment, or decreased the TP-induced increase of E2, AMH and P level in supernatant of cultured human ovarian granulosa cells. Although TP treatment notably elevated the LH level in supernatant of cultured human ovarian granulosa cells, just XJCRTSZW treatment combined with overexpression of PINK1 observably antagonized the enhancement. Thus, we demonstrated that XJCRTSZW promotes the cell viability of GCs induced by TP.

XJCRTSZW suppresses TP-induced oxidative stress injury in vitro

Similar to the results shown *in vivo*, EV and XJCRTSZW treatment significantly enhanced the TP-induced the diminishment of SOD levels, which was further significantly elevated with XJCRTSZW combined with overexpression of PINK1 but prominently decreased with XJCRTSZW combined with inhibition of PINK1. On the contrary, EV and XJCRTSZW treatment observably diminished the TP-induced the elevation of MDA levels, which was further markedly reduced with XJCRTSZW combined with inhibition of PINK1 but prominently increased with XJCRTSZW combined with overexpression of PINK1 (Fig. 5A). Moreover, both the level of ROS and apoptosis rate of cultured human ovarian granulosa cells were notably increased with TP treatment, which were markedly antagonized with EV and XJCRTSZW treatment. XJCRTSZW treatment combined with inhibition or overexpression of PINK1 prominently enhanced or declined the level of ROS and apoptosis rate of cultured human ovarian granulosa cells compared to these with XJCRTSZW treatment respectively (Fig. 5B, C and D). Therefore, these results indicated that XJCRTSZW suppresses TP-induced oxidative stress injury *in vitro*.

XJCRTSZW facilitates TP-induced mitophagy via PINK1/ Parkin signaling pathway in vitro

The reduction of MMP induced by TP was markedly elevated with EV and XJCRTSZW treatment, and XJCRTSZW treatment combined with inhibition or overexpression of PINK1 prominently decreased or increased the MMP level compared to that with XJCRTSZW treatment respectively (Fig. 6A). Transmission electron microscopy showed that there was an increase of mitophagy numbers with EV and XJCRTSZW treatment compared to that in TP group. XJCRTSZW treatment combined with inhibition or overexpression of PINK1 reduced or enhanced the mitophagy numbers compared to that in TP+XJCRTSZW group (Fig. 6B). Although EV and XJCRTSZW treatment just enhanced the TP-induced the diminishment of the LCII/LCI expression, significantly reduced the TP-induced the elevation of the p62 expression. Besides, the relative protein expression of p62 was prominently increased or decreased with XJCRTSZW treatment combined with inhibition or overexpression of PINK1 compared to that in TP+XJCRTSZW group. Furthermore, EV and XJCRTSZW treatment further notably enhanced the TP-induced elevation of PINK1 and Parkin protein levels, which was further increased with XJCRTSZW

treatment combined with overexpression of PINK1 (Fig. 6C and D). In brief, we concluded that XJCRTSZW facilitates TP-induced mitophagy via PINK1/ Parkin signaling pathway *in vitro*.

Discussion

In the present study, adult female SD rats and human ovarian granulosa cell lines were treated with TP, and then treated with XJCRTSZW. We found that XJCRTSZW can ameliorate TP-induced oxidative stress through mitophagy both *in vivo* and *in vitro*. Mechanically, mitophagy mediated by PINK1/ Parkin signaling pathway is involved in this process both *in vivo* and *in vitro*.

TP has multiple pharmacological effects including anti-inflammatory, anti-arteriosclerosis and anti-tumor that has been widely used in clinic. However, a growing number of evidence has shown that TP can induce the severe reproductive toxicity both in animals and human beings. In the present study, the severe reproductive toxicity was also observed after TP treatment, as indicated by the seriously pathological symptoms, the diminishment of primary follicles and secondary follicles, as well as the enhancement of atretic follicles *in vivo*, which was in accordance with the previous study [11]. Moreover, XJCRTSZW treatment notably antagonized the TP-induced pathological symptoms and changes of primary follicles, secondary follicles and atretic follicles numbers. The hypothalamus-pituitary-ovary axis (HPOA) modulates ovarian function, female menstrual cycle and fertility function via the feedback regulation mechanism of hormones [12], thus the dysregulation of HPOA can result in female endocrine dysfunction and infertility [13]. Our results revealed that XJCRTSZW treatment significantly elevated the TP-induced the reduction of E2 and AMH, but decreased the TP-induced the enhancement of FSH and LH. E2 is the most abundant and active estrogen in women. It is secreted by follicular granulosa cells and regulated by LH and FSH, which can promote the development of various organs of the reproductive system, facilitate endometrial hyperplasia and shedding, and maintain female secondary sexual characteristics [14]. AMH is secreted by the granular cells of small ovarian follicles, and its level is not affected by other exogenous hormone drugs or pregnancy. Thus, it is a reliable indicator for evaluating ovarian reserve and premature ovarian failure [15]. Both LH and FSH are secreted by the basophils of the anterior pituitary. Therein, FSH can facilitate the proliferation and differentiation of granulosa cells of the follicle, promote the maturation of the follicles, and make the ovaries grow. LH and FSH play a synergistic effect to promote the discharge of mature eggs, so that the ruptured follicles form a corpus luteum to secrete estrogen and progesterone [16]. Therefore, the levels of E2, AMH, LH, and FSH can directly reflect the functional status of the ovaries. Taken together, we demonstrated XJCRTSZW can ameliorate TP-induced reproductive toxicity via HPOA.

Plenty of studies have reported that TP can induce the oxidative stress response both *in vivo* and *in vitro* [7]. Similarly, our data showed that XJCRTSZW treatment significantly elevated the TP-induced the reduction of SOD, but decreased the TP-induced the enhancement of MDA and ROS levels both *in vivo* and *in vitro*. SOD is an antioxidant enzyme that specifically scavenges oxygen free radicals in the body that plays an important role in the body's oxidation and antioxidant balance, and can disproportionate superoxide anion free radicals to produce hydrogen peroxide to further convert into water by GSH-PX in

the body [17]. MDA is a degradation product of lipid peroxides, reflecting the peroxidation degree of body fat [17]. Thus, SOD activity and MDA content can indicate the degree of oxidative stress. Moreover, Cistanche [18], Cuscuta [19], Raspberry [20], Rehmannia [21], Caulis Spatholobi [22] and Eupatorium [23], the core composition of XJCRTSZW have been demonstrated the antioxidative role in various diseases. The elevated level of ROS can alter the balance between pro-oxidants and antioxidants, therefore, appropriate ROS is necessary for the normal cell progressions [24]. Excessive ROS induction is unfitted for normal female physiological reactions that in turn results in a series of reproductive diseases, such as PCOS, endometriosis and infertility [24, 25]. Therefore, these results indicated that XJCRTSZW can ameliorate TP-induced oxidative stress.

Our results also showed that XJCRTSZW treatment observably reduced the TP-induced the elevation of apoptosis rate both *in vivo* and *in vitro*. Except for apoptosis, autophagy can also be activated primarily in GCs [7]. Moreover, emerging evidence exhibits autophagic death is activated under oxidative stress conditions without inducing apoptosis in several mammalian cells [26, 27]. Our results showed that XJCRTSZW treatment markedly increased the number of mitophagy, and XJCRTSZW treatment also prominently enhanced the TP-induced the diminishment of ATP and MMP levels. Moreover, XJCRTSZW treatment significantly elevated the level of LCII/LCI, PINK1 and Parkin, while reduced the expression of p62 compared with TP treatment both *in vivo* and *in vitro*. Mitophagy is trigged upon the mitochondria is damaged, which can protect cells from different cytotoxic stimuli through the elimination of dysfunctional mitochondria [28]. As a mitochondrial serine/threonine protein kinase, PINK1 acts as a core role in modulating mitochondrial dynamics, trafficking, and quality control [29, 30]. Parkin is the E3 ubiquitin ligase that is also identified as a pivotal regulator of mitochondrial quality control. Moreover, Parkin can promote the PINK1-directed autophagic clearance of depolarized mitochondria [31, 32]. PINK1 tends to be steady on damaged mitochondria to activate Parkin because the reduction of MMP prevents proteasomal degradation of PINK1. Furthermore, in the present study, XJCRTSZW treatment combined with inhibition of PINK1 notably increased the apoptosis rate, the level of ROS, MDA and p62, while decreased the level of SOD, MMP, LCII/LCI, PINK1 and Parkin. On the contrary, XJCRTSZW treatment combined with overexpression of PINK1 markedly reversed these changes. In addition, previous study has shown that superfluous mitophagy can remove plentiful mitochondria, thereby causing apoptosis [33–35]. Also, mitophagy can be activated by oxidative stress [36]. Therefore, we concluded that XJCRTSZW facilitates TP-induced mitophagy via PINK1/ Parkin signaling pathway.

Conclusion

Our results exhibited that XJCRTSZW can ameliorate TP-induced oxidative stress through mitophagy both *in vivo* and *in vitro*. Mechanically, mitophagy mediated by PINK1/ Parkin signaling pathway is involved in this process both *in vivo* and *in vitro*.

Abbreviations

XJCRTSZW

XinJiaCongRongTuSiZiWan
POF
Premature ovarian failure
PCOS
Polycystic ovary syndrome
TP
Triptolide
PCD
Programmed cell death
GCs
Granulosa cells
PINK1
PTEN-induced kinase 1
TCM
Traditional Chinese Medicine
EV
Estradiol valerate
H&E
Hematoxylin and eosin
ELISA
Enzyme-linked immunosorbent assay
E2
Estradiol
AMH
anti-Mullerian hormone
FSH
Follicle stimulating hormone
LH
Luteinizing hormone
P
Progesterone
MDA
Malondialdehyde
SOD
Superoxide dismutase
RT-qPCR
Reverse transcription-quantitative polymerase chain reaction analysis
BSA
Bovine Serum Albumin
ECL

Electrochemilluminescence
HPOA
Hypothalamus-pituitary-ovary axis.

Declarations

Ethics approval and consent to participate

All the procedures were executed severely according to the Board and Ethics Committee of Shaanxi University of Chinese Medicine (SUCMDL20210310008).

Consent for publication

All the authors approved the manuscript for publication.

Availability of data and materials

The data used to support the findings of this study are included in the article.

Conflicts of interest/Competing interests

The authors declared that there is no conflict of interest.

Funding

This work was supported by the Key scientific research project of Shaanxi Provincial Department of Education in 2021 (21JS017).

Authors' contributions

Jin Yan, Disi Deng and Keming Wu performed the research. Min Liu analyzed and interpreted of data. Disi Deng and Keming Wu designed the research. Jin Yan and Yeke Wu draw the mode pattern and collect relevant references. Writing - review &editing performed by Keming Wu. Jin Yan and Disi Deng wrote the paper.

Acknowledgements

Not application.

References

1. Chen SR, Dai Y, Zhao J, Lin L, Wang Y, Wang Y. A Mechanistic Overview of Triptolide and Celastrol, Natural Products from Tripterygium wilfordii Hook F. Front Pharmacol. 2018;9:104.
2. Song C, Wang Y, Cui L, Yan F, Shen S. Triptolide attenuates lipopolysaccharide-induced inflammatory responses in human endothelial cells: involvement of NF-κB pathway. BMC Complement Altern Med.

2019;19(1):198.
3. Song W, Liu M, Wu J, Zhai H, Chen Y, Peng Z. Preclinical Pharmacokinetics of Triptolide: A Potential Antitumor Drug. Curr Drug Metab. 2019;20(2):147–54.
4. Yuan K, Li X, Lu Q, Zhu Q, Jiang H, Wang T, et al. Application and Mechanisms of Triptolide in the Treatment of Inflammatory Diseases-A Review. Front Pharmacol. 2019;10:1469.
5. Chen X, Chen SL. A woman with premature ovarian failure induced by Tripterygium wilfordii Hook.f. gives birth to a healthy child. Fertil Steril. 2011;96(1):e19–21.
6. Wang K, Hu H, Cui W, Zhang X, Tang Q, Liu N, et al. Palliative effects of metformin on testicular damage induced by triptolide in male rats. Ecotoxicol Environ Saf. 2021;222:112536.
7. Xi C, Peng S, Wu Z, Zhou Q, Zhou J. Toxicity of triptolide and the molecular mechanisms involved. Biomed Pharmacother. 2017;90:531–41.
8. Agarwal A, Aponte-Mellado A, Premkumar BJ, Shaman A, Gupta S. The effects of oxidative stress on female reproduction: a review. Reprod Biol Endocrinol. 2012;10:49.
9. Li J, Su J, Guo Z. WU K. Wu Keming's experience in treating premature ovarian failure. Hunan Journal of Traditional Chinese Medicine. 2014;30(12):38–9.
10. Ke X, Wang M, Wu K. Experience of Prof.WU Ke-ming for treatingPCOS in the integrative medicine. Clinical Journal of Chinese Medicine. 2015(1):91–2.
11. Liu J, Jiang Z, Liu L, Zhang Y, Zhang S, Xiao J, et al. Triptolide induces adverse effect on reproductive parameters of female Sprague-Dawley rats. Drug Chem Toxicol. 2011;34(1):1–7.
12. Wang F, Zhang ZH, Xiao KZ, Wang ZC. Roles of Hypothalamic-Pituitary-Adrenal Axis and Hypothalamus-Pituitary-Ovary Axis in the Abnormal Endocrine Functions in Patients with Polycystic Ovary Syndrome. Zhongguo Yi Xue Ke Xue Yuan Xue Bao. 2017;39(5):699–704.
13. Mikhael S, Punjala-Patel A, Gavrilova-Jordan L. Hypothalamic-Pituitary-Ovarian Axis Disorders Impacting Female Fertility. Biomedicines. 2019;7(1).
14. Nazari E, Suja F. Effects of 17β-estradiol (E2) on aqueous organisms and its treatment problem: a review. Rev Environ Health. 2016;31(4):465–91.
15. Suardi D, Permadi W, Djuwantono T, Hidayat YM, Bayuaji H, Edo Gautama GP. Correlation of Serum Anti-Mullerian Hormone (AMH) Level on Ovarian Volume in Women with Endometrioma. Int J Gen Med. 2021;14:1–8.
16. Palermo R. Differential actions of FSH and LH during folliculogenesis. Reprod Biomed Online. 2007;15(3):326–37.
17. Askari M, Mozaffari H, Darooghegi Mofrad M, Jafari A, Surkan PJ, Amini MR, et al. Effects of garlic supplementation on oxidative stress and antioxidative capacity biomarkers: A systematic review and meta-analysis of randomized controlled trials. Phytother Res. 2021.
18. Mehanna ET, El-Sayed NM, Ibrahim AK, Ahmed SA, Abo-Elmatty DM. Isolated compounds from Cuscuta pedicellata ameliorate oxidative stress and upregulate expression of some energy regulatory genes in high fat diet induced obesity in rats. Biomed Pharmacother. 2018;108:1253–8.

19. Hu Y, Huang J, Li Y, Jiang L, Ouyang Y, Li Y, et al. Cistanche deserticola polysaccharide induces melanogenesis in melanocytes and reduces oxidative stress via activating NRF2/HO-1 pathway. J Cell Mol Med. 2020;24(7):4023–35.
20. Garcia G, Nanni S, Figueira I, Ivanov I, McDougall GJ, Stewart D, et al. Bioaccessible (poly)phenol metabolites from raspberry protect neural cells from oxidative stress and attenuate microglia activation. Food Chem. 2017;215:274–83.
21. Yang YH, Yang H, Li RF, Li CX, Zeng L, Wang CJ, et al. A Rehmannia glutinosa cinnamate 4-hydroxylase promotes phenolic accumulation and enhances tolerance to oxidative stress. Plant Cell Rep. 2021;40(2):375–91.
22. Park HR, Lee H, Lee JJ, Yim NH, Gu MJ, Ma JY. Protective Effects of Spatholobi Caulis Extract on Neuronal Damage and Focal Ischemic Stroke/Reperfusion Injury. Mol Neurobiol. 2018;55(6):4650–66.
23. Melo AS, Monteiro MC, da Silva JB, de Oliveira FR, Vieira JL, de Andrade MA, et al. Antinociceptive, neurobehavioral and antioxidant effects of Eupatorium triplinerve Vahl on rats. J Ethnopharmacol. 2013;147(2):293–301.
24. Ruder EH, Hartman TJ, Goldman MB. Impact of oxidative stress on female fertility. Curr Opin Obstet Gynecol. 2009;21(3):219–22.
25. Al-Gubory KH, Fowler PA, Garrel C. The roles of cellular reactive oxygen species, oxidative stress and antioxidants in pregnancy outcomes. Int J Biochem Cell Biol. 2010;42(10):1634–50.
26. Pan X, Liu D, Wang J, Zhang X, Yan M, Zhang D, et al. Peneciraistin C induces caspase-independent autophagic cell death through mitochondrial-derived reactive oxygen species production in lung cancer cells. Cancer Sci. 2013;104(11):1476–82.
27. Chen Y, McMillan-Ward E, Kong J, Israels SJ, Gibson SB. Oxidative stress induces autophagic cell death independent of apoptosis in transformed and cancer cells. Cell Death Differ. 2008;15(1):171–82.
28. Laker RC, Drake JC, Wilson RJ, Lira VA, Lewellen BM, Ryall KA, et al. Ampk phosphorylation of Ulk1 is required for targeting of mitochondria to lysosomes in exercise-induced mitophagy. Nat Commun. 2017;8(1):548.
29. Chu CT. A pivotal role for PINK1 and autophagy in mitochondrial quality control: implications for Parkinson disease. Hum Mol Genet. 2010;19(R1):R28–37.
30. Pickrell AM, Youle RJ. The roles of PINK1, parkin, and mitochondrial fidelity in Parkinson's disease. Neuron. 2015;85(2):257–73.
31. Vives-Bauza C, Zhou C, Huang Y, Cui M, de Vries RL, Kim J, et al. PINK1-dependent recruitment of Parkin to mitochondria in mitophagy. Proc Natl Acad Sci U S A. 2010;107(1):378–83.
32. Geisler S, Holmström KM, Skujat D, Fiesel FC, Rothfuss OC, Kahle PJ, et al. PINK1/Parkin-mediated mitophagy is dependent on VDAC1 and p62/SQSTM1. Nat Cell Biol. 2010;12(2):119–31.
33. Su SH, Wu YF, Wang DP, Hai J. Inhibition of excessive autophagy and mitophagy mediates neuroprotective effects of URB597 against chronic cerebral hypoperfusion. Cell Death Dis.

2018;9(7):733.

34. Marycz K, Kornicka K, Szlapka-Kosarzewska J, Weiss C. Excessive Endoplasmic Reticulum Stress Correlates with Impaired Mitochondrial Dynamics, Mitophagy and Apoptosis, in Liver and Adipose Tissue, but Not in Muscles in EMS Horses. Int J Mol Sci. 2018;19(1).
35. Lu J, Shen Y, Liu LJ, Qian HY, Zhu CL. Combining Epinephrine and Esmolol Attenuates Excessive Autophagy and Mitophagy in Rat Cardiomyocytes After Cardiac Arrest. J Cardiovasc Pharmacol. 2015;66(5):449–56.
36. Yang YH, Li B, Zheng XF, Chen JW, Chen K, Jiang SD, et al. Oxidative damage to osteoblasts can be alleviated by early autophagy through the endoplasmic reticulum stress pathway–implications for the treatment of osteoporosis. Free Radic Biol Med. 2014;77:10–20.

Table

Table 1 is not available with this version

Figures

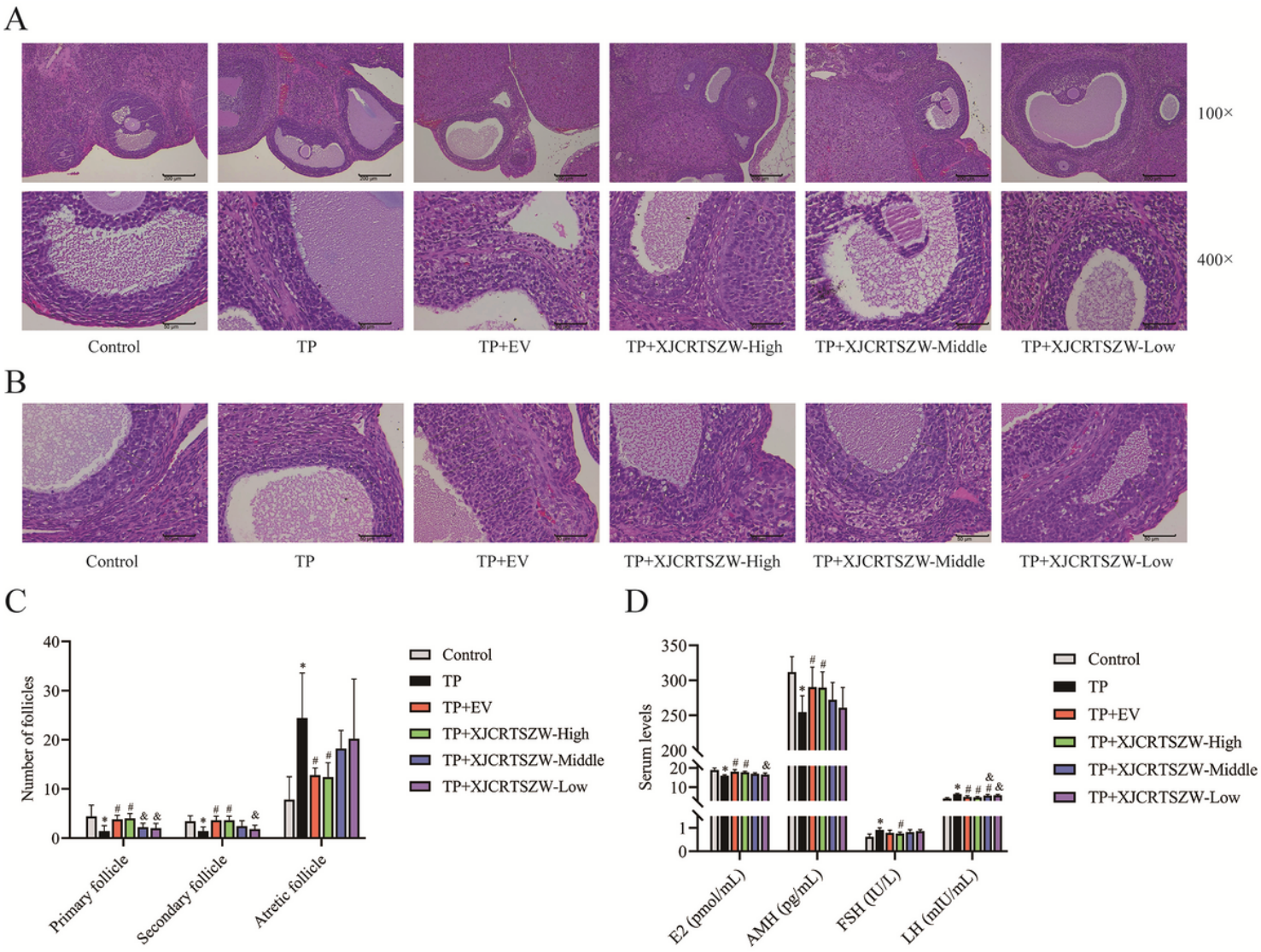

Figure 1

XJCRTSZW ameliorates TP-induced reproductive toxicity. (A) Histological analysis of ovary was determined by H&E stain. (B) The number of primary follicles, secondary follicles and atretic follicle was measured after ovary was stained with H&E. (C) The serum level of E2, AMH, LNH-B, FSH and LH was detected using commercial ELISA kits. The means ± SD of five independent samples were shown. *p < 0.05 compared to control group. #p < 0.05 compared to TP group. &p < 0.05 compared to TP+XJCRTSZW-High group.

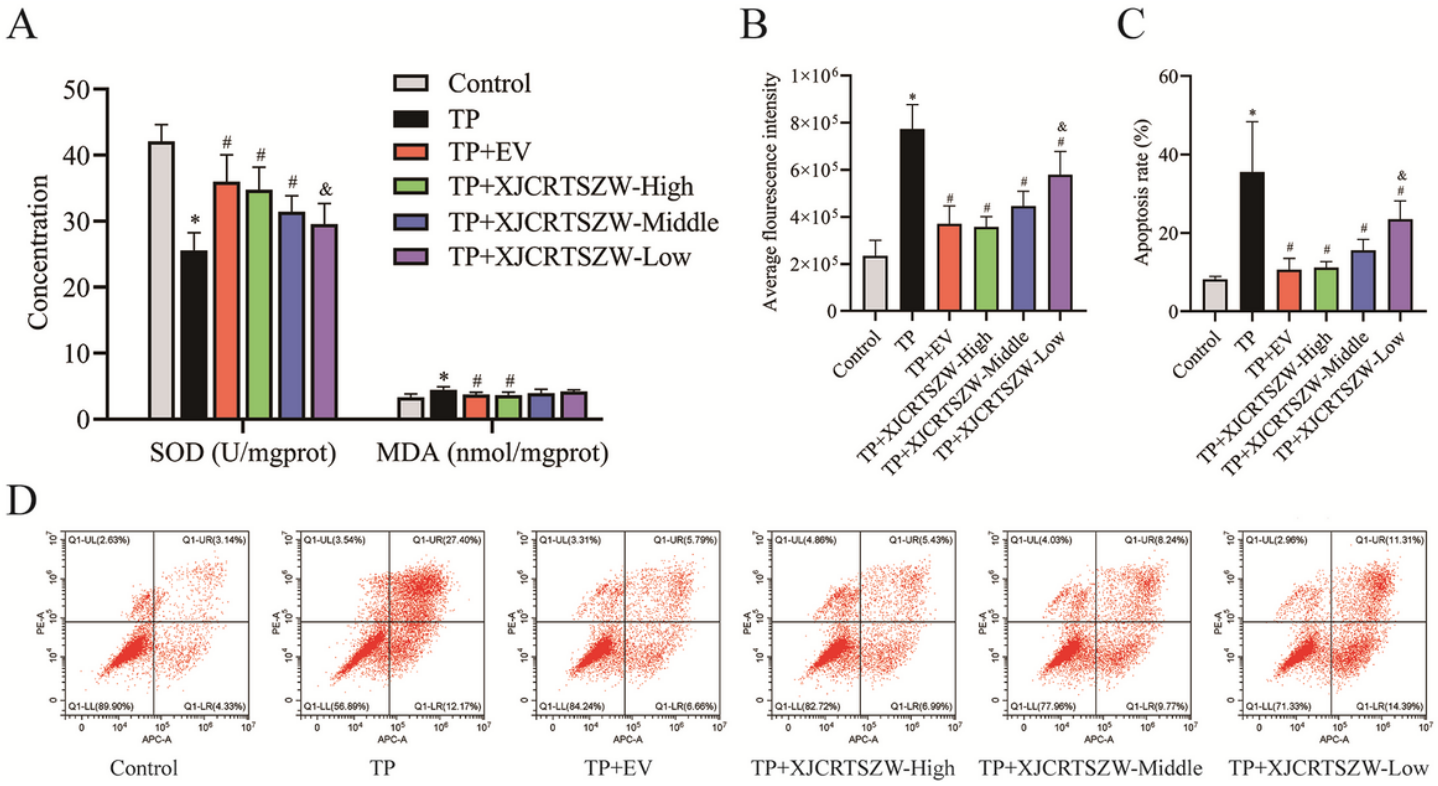

Figure 2

XJCRTSZW inhibits TP-induced oxidative stress injury and apoptosis in vivo. (A) The level of SOD and MDA in GCs was detected using commercial kits. (B) The ROS level was determined using reactive oxygen species assay kit and the fluorescence of the cells was measured by flow cytometry. (C and D) The apoptosis rate was analyzed using flow cytometry assay. The means ± SD of five independent samples were shown. *p < 0.05 compared to control group. #p < 0.05 compared to TP group. &p < 0.05 compared to TP+XJCRTSZW-High group.

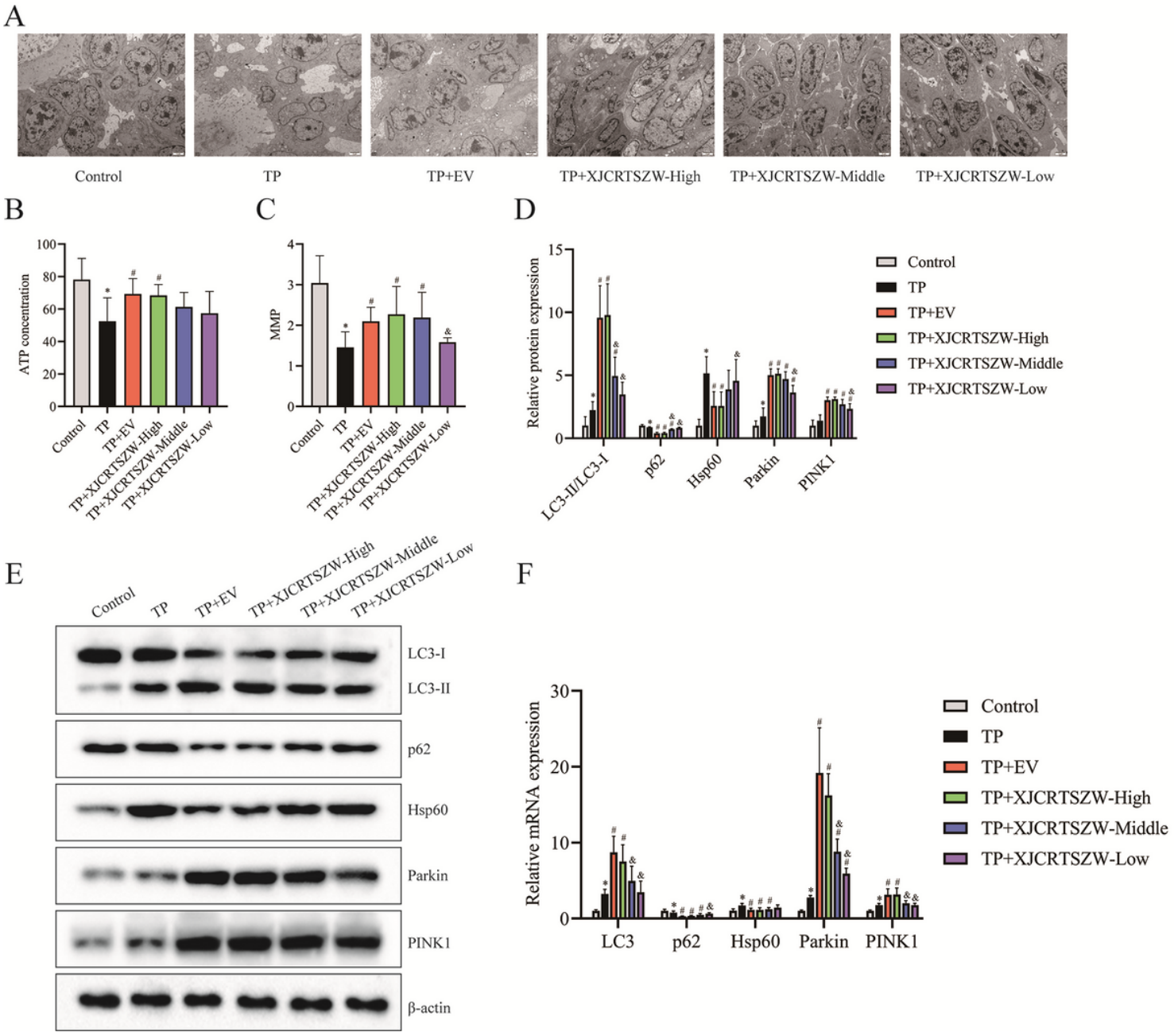

Figure 3

XJCRTSZW promotes TP-induced mitophagy via PINK1/ Parkin signaling pathway in vivo. (A) The mitophagy in GCs was assessed using transmission electron microscope. (B) The level of ATP was detected by ELISA assay. (C) MMP was determined by JC-1 staining. (D and E) The protein level of LC3-Ⅱ/LC3-Ⅰ, p62, Hsp60, Parkin and PINK1 was evaluated using western blot. The data were expressed after being normalized to β-actin. (F) The mRNA level of LC3, p62, Hsp60, Parkin and PINK1 was detected using qRT-PCR. The data were expressed after being normalized to β-actin. The means ± SD of five independent samples were shown. *p < 0.05 compared to control group. #p < 0.05 compared to TP group. &p < 0.05 compared to TP+XJCRTSZW-High group.

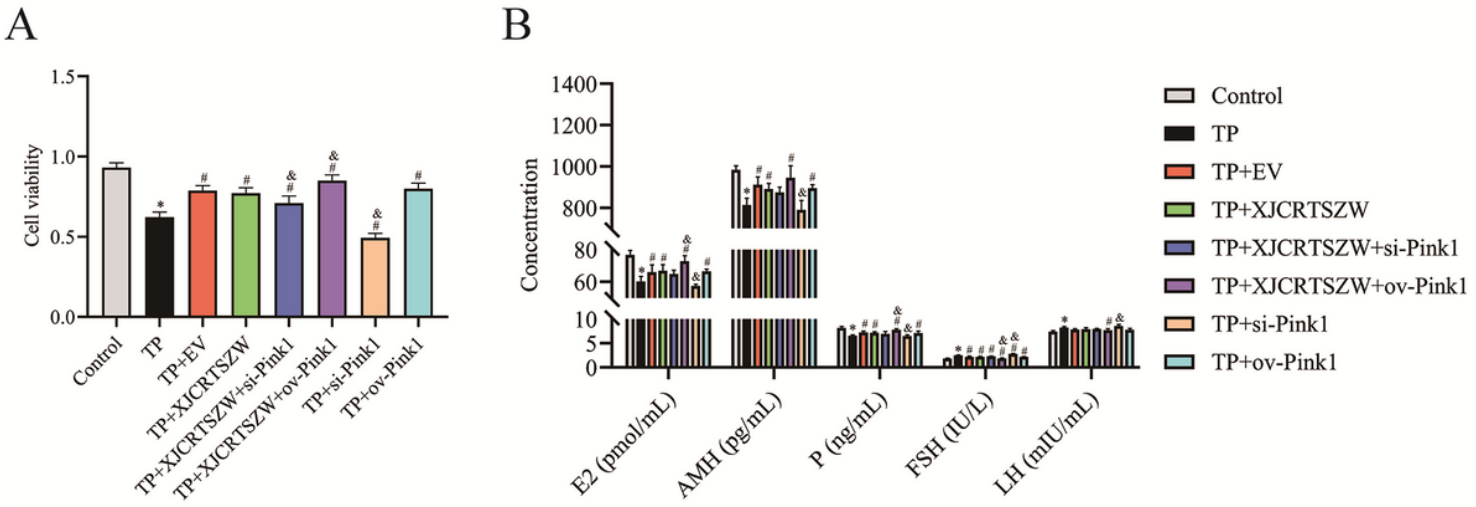

Figure 4

XJCRTSZW promotes the cell viability of GCs induced by TP. (A) Cell viability was detected using CCK-8. (B) The level of E2, AMH, P, FSH and LH level in supernatant of cultured human ovarian granulosa cells was determined using commercial ELISA kits. The means ± SD of three independent samples were shown. *p < 0.05 compared to control group. #p < 0.05 compared to TP group. &p < 0.05 compared to TP+XJCRTSZW group.

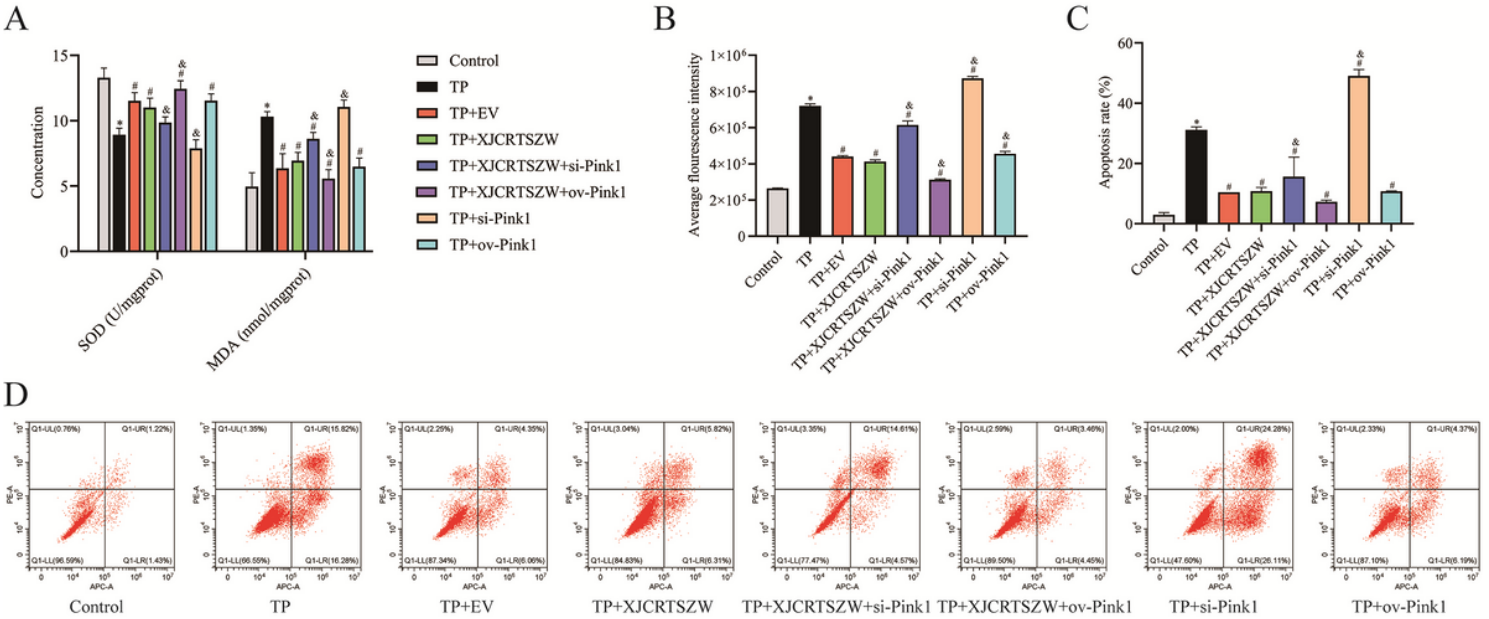

Figure 5

XJCRTSZW suppresses TP-induced oxidative stress injury in vitro. (A) The level of SOD and MDA in GCs was detected using commercial kits. (B) The ROS level was determined using reactive oxygen species assay kit and the fluorescence of the cells was measured by flow cytometry. (C and D) The apoptosis rate was analyzed using flow cytometry assay. The means ± SD of three independent samples were shown. *p < 0.05 compared to control group. #p < 0.05 compared to TP group. &p < 0.05 compared to TP+XJCRTSZW group.

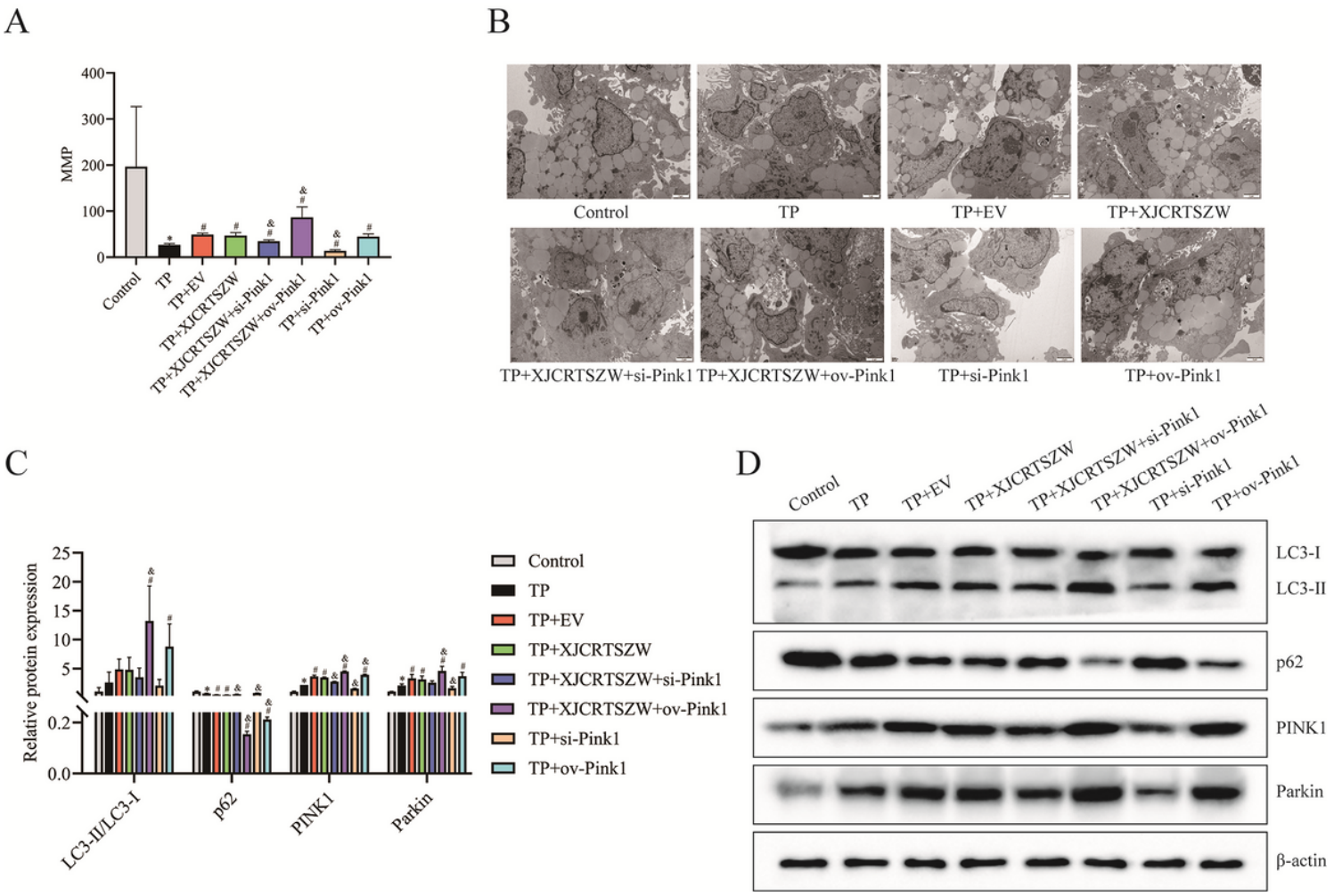

Figure 6

XJCRTSZW facilitates TP-induced mitophagy via PINK1/ Parkin signaling pathway in vitro. (A) MMP was determined by JC-1 staining. (B) The mitophagy in GCs was detected using transmission electron microscope. (C and D) The protein level of LC3-Ⅱ/LC3-Ⅰ, p62, Parkin and PINK1 was evaluated using western blot. The data were expressed after being normalized to β-actin. The means ± SD of three independent samples were shown. *p < 0.05 compared to control group. #p < 0.05 compared to TP group. &p < 0.05 compared to TP+XJCRTSZW group.